Combined PET/MRS brain studies show dynamic and long-term physiological changes in a primate model of Parkinson disease

ANNA-LIISA BROWNELL[1,3], BRUCE G. JENKINS[1], DAVID R. ELMALEH[1], TERRENCE W. DEACON[3], ROGER D. SPEALMAN[4] & OLE ISACSON[2,3]

[1]Department of Radiology and [2]Neurology, Massachusetts General Hospital, and Program in Neuroscience Harvard Medical School, Boston, Massachusetts 02114, USA [3]Neuroregeneration Laboratories, McLean Hospital, Belmont, Massachusetts 02178, USA

[4]New England Regional Primate Research Center, Southborough, Massachusetts 01772, USA

Correspondence should be addressed to O.I.

We used brain imaging to study long-term neurodegenerative and bioadaptive neurochemical changes in a primate model of Parkinson disease. We gradually induced a selective loss of nigrostriatal dopamine neurons, similar to that of Parkinson disease, by creating oxidative stress through infusion of the mitochondrial complex 1 inhibitor MPTP for 14 ± 5 months. Repeated evaluations over 3 years by positron emission tomography (PET) demonstrated progressive and persistent loss of neuronal dopamine pre-synaptic re-uptake sites; repeated magnetic resonance spectroscopy (MRS) studies indicated a 23-fold increase in lactate and macromolecules in the striatum region of the brain for up to 10 months after the last administration of MPTP. By 2 years after the MPTP infusions, these MRS striatal lactate and macromolecule values had returned to normal levels. In contrast, there were persistent increases in striatal choline and decreases in N-acetylaspartate. Thus, these combined PET/MRS studies demonstrate patterns of neurochemical changes that are both dynamic and persistent long after selective dopaminergic degeneration.

In neurological diseases like Parkinson disease (PD), examination of the living brain by high resolution positron emission tomography (PET) and magnetic resonance imaging (MR), combined with the appropriate pharmaco-kinetic and physiological analyses, can provide valuable quantitative information of altered brain function[1,2]. Imaging technology depends on the limits of imaging (resolution and sensitivity) as well as biological variables (tissue structure and biochemical processes)(refs. 3–6). In applications involving the human brain, recent progress in obtaining localized magnetic resonance spectra (MRS) and spectroscopic images has made possible new studies of tumors[7,8] and infarcts[9,10], as well as examination of normal brain physiology[11].

The most prominent pathological change in idiopathic Parkinson disease is degeneration of the nigrostriatal-dopaminergic pathway associated with severe cell loss in the substantia nigra[12]. In patients, a chief consequence of the loss of dopamine (DA) neurons is a substantial decrease in the density of dopaminergic synapses and in the concentrations of DA in the striatum[13,14]. The striatal loss of DA results in typical signs, including akinesia, bradykinesia, rigidity and resting tremor. These findings led to experiments aimed at developing animal models of PD using neurotoxins; such as 6-hydroxydopamine[15,16], selective for DA neurons. Some cases of parkinsonism have developed after accidental intravenous self-administration of a meperidine analogue; 1-methyl-4-phenyl-1,2,3,6 tetrahydropyridine[17] (MPTP). The affected individuals had symptoms that included severe akinesia, rigidity, flexed posture and a resting tremor. The symptoms were associated with decreased striatal ^{18}F-fluoro-L-dopa uptake, observed using PET[18], and considerable loss of pigmented neurons in the substantia nigra.

In primates, administration of MPTP by stereotaxic application in the striatum, intra-carotid injections or repeated intravenous injection over 5–10 days[19–21] generally induces a substantial DA depletion resulting in a severe akineto-rigid PD syndrome (often requiring drug therapy) within weeks after administration of the neurotoxin. In contrast, repeated low-dose administration of MPTP over a longer period of time (up to 19 months) increases the selectivity of the neurotoxin for specific subpopulations of DA neurons, more accurately reproducing the pattern of neuropathological and neurochemical alterations observed in idiopathic PD[22,23]. In this chronic administration model, and in idiopathic PD[5,24], signs develop gradually, and after these signs appear they do not spontaneously recover as reported in some acute MPTP models[25]. This animal model therefore represents a stable parkinsonian syndrome, which is necessary for the exploration of long-term functional changes and experimental therapies.

The ability of MRS to sensitively measure neurochemicals in brain volumes less than 1 ml provides a unique 'window' into neurodegenerative processes. MRS is especially useful because it allows quantification of different chemicals in a single study, which can be repeated many times. Chemicals quantifiable in proton MRS include N-acetyl aspartate (NAA), a correlate marker for healthy mature neurons[26,27]. Thus, MRS has been used to study neuronal loss, using NAA as a marker[28–31]. Loss of NAA may not always correlate with the final destruction of

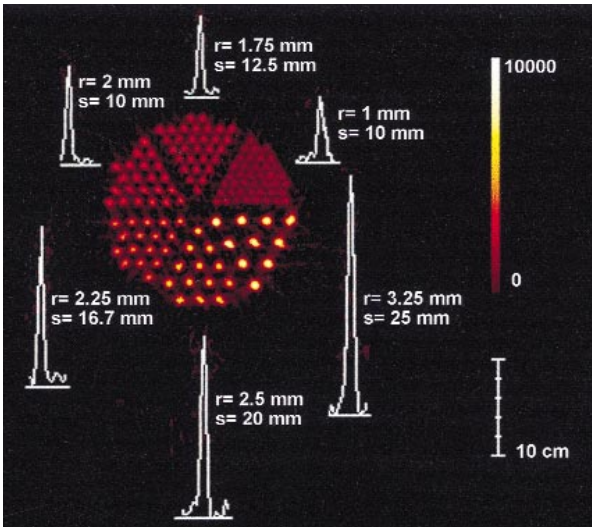

Fig. 1 PCR-I with ^{18}F-labeled water in a 'Derenzo-phantom'. PCR-I is a high-resolution brain imaging device; the phantom is a solid plastic disk with six sectors of holes each of a different radius (r) and separations (s). There is uniform distribution of radioactivity in all the sectors, with clearly separated images even for holes 2.0 mm in diameter with 10-mm separation. Spectra next to each sector describe measured count distribution in a single hole in each sector corresponding a volume of $3.14 \times (r)^2 \times 5$ mm^3 (the thickness of the slice is 5 mm). Scale bar represents 10 cm, with each division being 2 cm.

neurons, but to some degree may reflect their health[32,33]. In addition to NAA, substances such as lactate, glutamate, creatine, choline and myo-inositol provide a view of the progression of neurodegeneration; for example, in gliosis, glial cells have a concentration of cholines (trimethylamines) twice that of neurons[27]. Elevated choline concentrations are also found in conditions involving the proliferation of pathological forms of glial cells such as gliomas[7,8]. The main limitation in using MRS is its relative insensitivity compared to PET, because of the low signal obtained per molecule. NAA, the most prominent molecule in a brain proton spectrum, has an approximate concentration of 8–10 mM in the brain. Even at this concentration, MRS yields a low signal-to-noise ratio, which leads to a relatively low spatial resolution. Recent developments in PET instrument design have greatly improved the performance of PET[34,35]. Theoretically, the resolution of PET is limited by three factors: positron range, small angle deviation, and the sampling achieved by the detectors. For these experiments, positron emission tomography studies were done using a PET scanning system (PCR-I) equipped with one ring of 360 BGO (bismuth germanate) detectors and a computer controlled imaging table[36]. Here we have studied the long-term physiological changes after MPTP-induced neurotoxicity using PET and MRS techniques, in a primate model of PD.

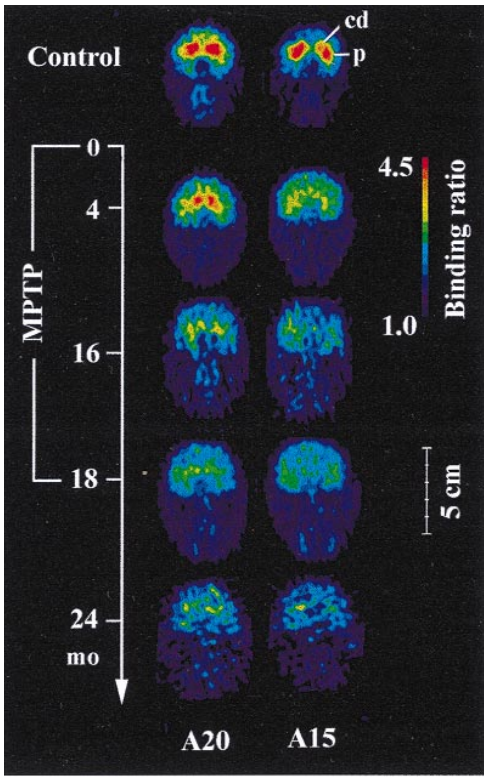

Functional PET studies

Using a specially adapted PET scanning system (Fig. 1), we investigated chronic neurodegenerative processes over 3 years in a Parkinson disease model in five cynomolgus monkeys (Macaca fascicularis). We used carbon-11-labeled 2β-carbomethoxy-3β-(4-fluorophenyl) tropane (^{11}C-CFT, or WIN 35,428) as a tracer for visualizing dopamine re-uptake sites located on presynaptic dopamine terminals in experimental animals. We compared regional accumulation of ^{11}C-CFT in the striatum at two different coronal brain levels (A20 and A15 from the stereotaxic zero) with its accumulation in the cerebellum in the weeks before, during and after administration of MPTP; this treatment produces a parkinsonian brain degeneration of the dopamine system (Fig. 2). The striatal-to-cerebellar ratio of the ^{11}C-CFT accumulation was 4.5 in the pre-MPTP study and declined with the onset of MPTP administration. Spontaneous locomotor activity decreases in parallel with the decline of the ^{11}C-CFT uptake[23]; however, overt Parkinsonian signs appear only after locomotor activity and the ^{11}C-CFT uptake rate decline to about 30% of their pre-MPTP values[23]. Here the putaminal binding potential of ^{11}C-CFT continues to decline 5–8 months after termination of MPTP administration (Fig. 2) and remains at this level for 2 years after MPTP treatment (Fig. 3). Similarly, the ^{11}C-CFT levels in caudate continued to decline from 55% when MPTP treatment was stopped (Fig. 2) to 21 ± 9% 5–8 months after its termination, and remained at this level for 2 years (Fig. 3). Thus, functional degeneration of DA terminals continues for approximately 5–8 months after MPTP treatment ends and then does not spontaneously recover. During MPTP administration, ^{11}C-CFT accumulation decreased at a faster rate in putamen than in caudate (as seen in PD)(Figs. 2 and 3), indicating that DA terminals are more sensitive to MPTP in the putamen than in the caudate.

MRS studies during neural degeneration

We used ^{1}H water-suppressed MRS to measure biochemical changes in the striatum during MPTP-induced neurodegenera-

Fig. 2 A long-term follow-up study of comparative distribution of ^{11}C-CFT in a primate Parkinson disease model. Two representative coronal brain levels (A20 and A15) are presented before (0), during (4,16,18) and 6 months after (24) MPTP treatment. Images are normalized to cerebellar activity and represent distribution of specific to nonspecific binding of ^{11}C-CFT in the brain 60–62 min after administration of the labeled ligand.

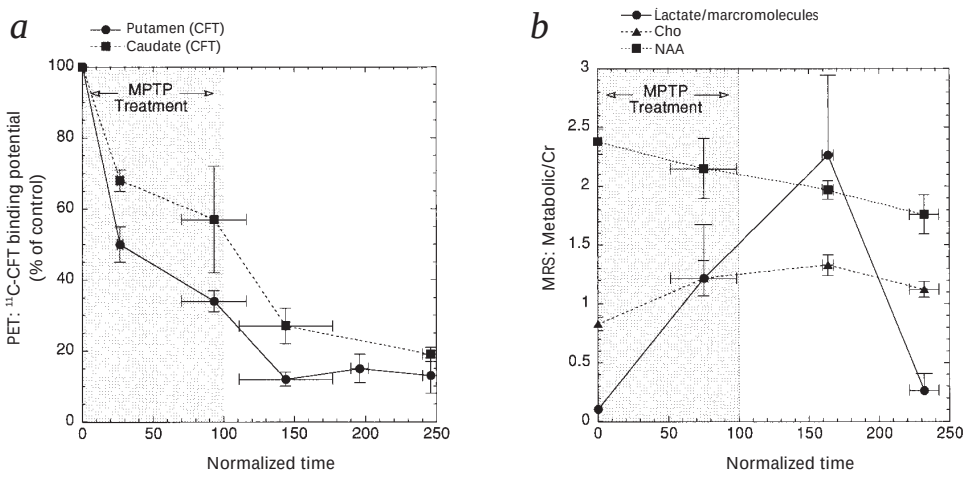

Fig. 3 PET studies of ^{11}C-CFT binding (***a***) and MRS studies of striatal biochemistry (***b***) before, during and after MPTP-induced neurotoxicity. There were irreversible changes of ^{11}C-CFT binding, choline and N-acetylaspartate concentration, as well as a 23-fold increase in peaks corresponding to lactate and macromolecule concentration that was reversible. Normalized time scale (horizontal axis) is obtained based on the response to MPTP-induced neurotoxicity in individual monkeys (as in patients, susceptibility varies). When the monkey showed overt parkinsonian symptoms, MPTP was terminated. The time of the MPTP treatment was normalized to 100, and the follow-up period was also normalized for each animal according this scale. The control value of the binding potential (k_3/k_4) was normalized to 100 and all the follow-up values were also normalized using this scale. The average follow-up time post MPTP was 2 years and the average value of the binding potential in control studies was 4.6–5.6 in putamen and 4.8 –6.6 in caudate region of the striatum.

tive processes. Complementary studies of DA re-uptake sites by PET and neurochemical changes by MRS are shown before MPTP treatment and 2 months after the last MPTP administration (Fig. 4). MPTP induced elevation of lactate/macromolecules and choline peaks (Figs. 3 and 4). Even as much as 10 months after termination of MPTP-induced neurotoxicity, the elevation in lactate/macromolecular peak was 23-fold ± 7-fold (Fig. 3). The choline/creatine (Cho/Cr) ratio in control monkeys was 0.83 ± 0.06 (Fig. 4), whereas it was 1.30 ± 0.15 in the 8–10 months after MPTP-induced neurotoxicity (Figs. 3 and 4). The NAA/Cr ratio in the control monkeys had very high inter-animal reproducibility (2.38 ± 0.11). This ratio decreased slightly but significantly in MPTP-treated monkeys to 1.93 ± 0.21 ($P < 0.01$) in the striatum 8–10 months after termination of MPTP treatment. This finding may reflect that MPTP is mostly neurotoxic for dopaminergic neurons in the substantia nigra, with only transsynaptic anterograde degeneration of the striatum[37,38]. Our data also show that the changes in NAA and Cho persisted after MPTP-induced neurotoxicity (Fig. 3). Two years after MPTP treatment stopped, the increase of choline in treated monkeys was 38 ± 4 % of the control value, and the corresponding decrease of NAA was 26 ± 4 % (Fig. 3). In contrast, the changes in lactate /macromolecular signal are reversible; by 2 years after final MPTP administration, this value had returned to control (background) levels. At approximately the time the striatal level of DA reuptake sites (^{11}C-CFT) reached a minimum in PET studies, the lactate peak seen with MRS reached a maximum.

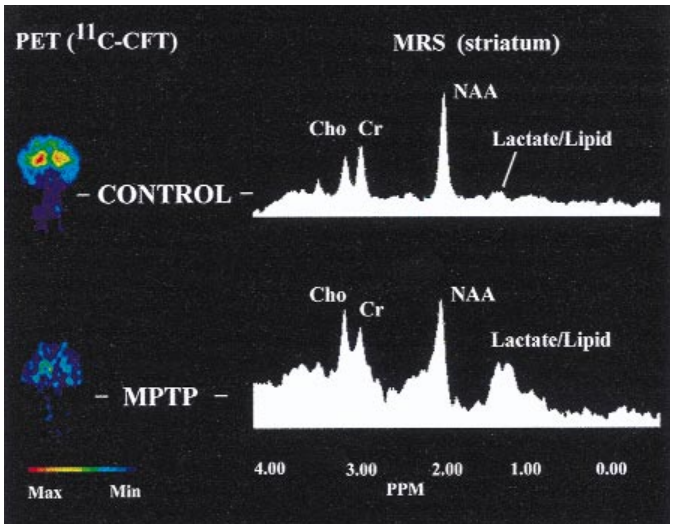

Fig. 4 PET and MRS studies of a monkey before any MPTP and 2 months after the last MPTP treatment. PET images (left) demonstrate that specific/nonspecific binding ratio of ^{11}C-CFT was considerably decreased after MPTP treatment (color coded by Max–Min bar at bottom). MRS (right) demonstrates a decreased NAA/Cr ratio, an elevated Cho/Cr ratio and an elevated lactate and macromolecule peak after MPTP treatment (TR/TE 2000/272 ms; PRESS).

Discussion

These experiments demonstrate, through the combined use of PET and MRS methods, a dynamic and specific neurochemical pattern of long-term neurodegenerative changes in the primate striatum after DA loss similar to that of PD. The physiological changes characterized by this combined PET/MRS approach provide data for a comprehensive *in vivo* analysis of the ongoing biological processes occurring after selective neural degeneration.

In animal models[22,23] and in humans[39], ^{11}C-CFT is a useful ligand to monitor DA terminal degeneration by PET scanning[23]. CFT was the first ligand to demonstrate a loss of DA fiber density equivalent to the loss of DA in human post-mortem Parkinson-diseased brains[40]. ^{11}C-CFT binding also correlates with motor signs in the MPTP primate model of Parkinson disease[22]; these observations have been verified in a larger series of primates[23] and are analogous with findings in early Parkinson disease in humans[40].

Here we studied ^{11}C-CFT levels and biochemical parameters in the striatum of each monkey for about 2 years after the monkey developed overt parkinsonian signs (at which time MPTP treatment was terminated). These data show persistent long-term physiological changes in striatal CFT binding and MRS-identified levels of choline and NAA. The changes in NAA and

choline levels were moderate and are consistent with an interpretation that MPTP-induced neuronal loss is mostly in the substantia nigra and that transsynaptic anterograde degeneration is in striatum[37,41]. MRS studies in patients with idiopathic Parkinson disease show few changes in striatal NAA or choline, but decreases of NAA and increase of choline are seen in some forms of parkinsonism[42,43].

We noted large changes in the MR spectral region between 1 ppm and 1.5 ppm (corresponding to lactate and macromolecules). Before the oxidative stress induced by MPTP, the intensity of this spectral band in the striatum was at background level, but with MPTP treatment, several large selective increases in striatal signal intensity were observed. First, there was a large increase of intensity at 1.33 ppm consistent with elevations in lactate (Fig. 3). After termination of MPTP treatment, there were even larger increases in signals at both 1.0 and 1.3–1.5 ppm. These later changes may reflect ongoing oxidative stress caused by physiological adaptive changes in function of the striatum. The presence of large amounts of mobile lipids acutely after MPTP treatment provides evidence for neuronal membrane breakdown possibly caused by lipid peroxidation or cell death mediated through cellular respiratory-chain inhibition[10,38]. However, the molecular species involved have not yet been specifically identified[10,38]. Detailed histological analysis of the striatum, however, indicates very little macrophage infiltration or gliosis in the MPTP-treated striatum in this progressive MPTP-induced degeneration[20,22]. Nonetheless, minor local striatal neuronal loss around large blood vessels and arterioles has been observed (O.I. and N.K. Kowall, unpublished observation), probably a consequence of direct MPTP-induced neuronal degeneration and mild gliosis from high toxin levels next to blood vessels (from intravenous administration of MPTP). The changes in the lactate and macromolecular peaks are reversible, however, and return to baseline 2 years after termination of MPTP administration.

These dynamic neurochemical shifts that occur several years after the neurotoxic event may relate to important physiological and pathological processes. For example, the signs of PD are not discernable in a patient until there is a 60–80% decrease in striatal dopamine levels. This in itself indicates fundamental adaptive physiological processes that maintain striatal function despite considerable degeneration of one transmitter system. Beyond this critical threshold, PD unfolds in a movement disorder that can, at least initially, be reversed by DA drug replacement therapy. Because the results of the MPTP treatment used here closely resemble the DA degeneration seen in PD, the movement disorder in this primate model also develops at the critical threshold of DA loss[22,23]. The dynamic and persistent physiological changes seen here using PET and MRS may therefore reflect similar adaptive striatal responses to those occurring in PD. Furthermore, the oxidative stress seen years after the neurotoxic events leading to DA loss indicate that the striatal neuronal circuitry may be compromised and at risk for subsequent structural and pathological processes. Future investigations should determine if such physiological stress of the caudate-putamen also occurs after other types of neurodegenerative events, or after long-term pharmacologically induced changes of the DA system[44].

These data indicate that the structural and neurochemical changes after a DA neurotoxic event are dynamic and complex, and continue to develop long after the neurodegenerative stimulus has stopped and PD signs develop. The characterization of these physiological changes may provide insights and a time frame for new therapeutic interventions in PD.

Methods

Primate model. The behavioral model of PD in cynomolgus monkeys (Macaca fascicularis) was produced by the chronic administration (0.6 mg/kg intravenously, every 2 weeks until behavioral stability) of the mitochondrial complex 1 inhibitor 1-methyl-4-phenyl-1,2,3,6-tetrahydropyridine[23] (MPTP). Spontaneous locomotor activity was quantified by continuous monitoring with four pairs of infrared motion detectors. Additional video recording and assessment was done monthly. Hypokinesia (decreased frequency of spontaneous movement), bradykinesia (slowness of movement) and tremor were rated by two independent observers to generate a clinical score (0–12), as reported[23]. Animals used in this study were maintained according to the guidelines of the Committee on Animals of the Harvard Medical School and Massachusetts General Hospital and those of the *Guide for Care and Use of Laboratory Animals* of the Institute of Laboratory Animal Resources, National Research Council, Department of Health, Education and Welfare.

PET techniques. The resolution of PCR-I for a point source at the center is 4.5 mm, and the sensitivity is 46,000 counts per s for a source 20 cm in diameter with a concentration of 1 μCi/ml. The overall detection efficiency of photons is 64% of the theoretical maximum for a plane thickness corresponding to the 2-cm-high detectors. A plane thickness of 5 mm (as used in this study) is obtained by limiting the effective height of detectors with cylindrical collimators, and it corresponds to a volume resolution of 0.08 ml. The resolving time of the PCR-I is 6 ns (FWHM).

We used a 'Derenzo-phantom' initially, with ^{18}F-labeled water as a radioactive tracer (Fig. 1). The phantom is a solid plastic disk with six sectors of holes of different diameters and separations. All the holes have the same length (25 mm). The smallest holes have a diameter of 2.0 mm and the separation between the midpoints of the holes is 10 mm. The largest holes have a diameter of 6.25 mm and the separation between the midpoints of these holes is 25 mm. Using the PCR-I, it is possible to image objects 2 mm in size separated by 1 cm (Fig. 1).

The synthesis of ^{11}C-CFT involves direct ^{11}C-methyl iodide methylation of 2β-carbomethoxy-3β-(-4-fluorophenyl)tropane (WIN 35,428; prepared by Organix, Woburn, Massachusetts) as published[45]. For PET imaging, monkeys were anaesthetized with 30mg/kg ketamine and 3mg/kg xylazine (initial dose, intramuscularly), and anesthesia was maintained with half this dose as needed. The femoral artery and vein were catheterized for collection of blood samples and injection of labeled ligand. The monkey was placed in the imaging position and the head was adjusted in a stereotaxic headholder with the earbar as a reference plane. Interior orbital supports ensure that images are acquired in pseudocoronal plane perpendicular to the orbito–meatal line. This allows superposition of data from MRI and MRS studies. After administration of labeled ligand (5 mCi; specific activity 600–1000 mCi/μmol) into the femoral vein, imaging data were collected 'stepwise' on seven coronal levels: A30 (that is, 30 mm anterior from the earbar), A25, A20, A15, A10, P5 (that is, 5 mm posterior from the earbar) and P10. The initial acquisition time per image was 15 s; it was subsequently increased to 60 s with the total imaging time being 90 min. Eighteen arterial blood samples of 0.1 ml each were drawn to monitor the decrease of radioactivity, starting a frequency of 15 s and ending with a frequency 15 min. In addition, six arterial samples were collected for HPLC analyses of metabolites of labeled ligand. Calibration of the positron tomograph was done for each study session, using the cylindrical plastic phantom (diam. 6 cm) and ^{18}F-labeled water. Cross-calibration with a gamma counter (Cobra Auto-gamma; Packard, Downers Grove, Illinois) was also done using ^{18}F-labeled water. Plasma data were corrected for counting efficiency, calibration factor and measured metabolites, and percent activity of the injected dose and ligand concentration were calculated. Imaging data were corrected for uniformity, sensitivity, attenuation, decay and collection time. PET images were reconstructed using Hanning weighted convolution backprojection[46]. Regions of interest (including left and right caudate and putamen, frontal cortex and cerebellum) were outlined from anatomical representations on the screen, and activity per unit volume, percent activity of the injected dose and ligand concentration were calculated. Data were analyzed using a three-compartmental model[39] and

SAAM program[47]. Plasma data were corrected for metabolites using an experimental two exponential correction function; $f(t) = 0.709 \times \exp(-0.108 \times t) + 0.286 \times \exp(-0.014 \times t)$. Binding potential was calculated as a ratio of transportation coefficients (k_3/k_4) into (k_3) and from (k_4) the area of interest (caudate or putamen).

MRS techniques. Monkeys were scanned on a GE 1.5T Sigma scanner (General Electric, Milwaukee, Wisconsin) using a saddle coil 15 cm in diameter. Monkeys were anesthesized with a dose of a mixture of 30 mg/kg ketamine and 3mg/kg xylazine. In the neurochemical analysis[30], single voxel spectra were recorded from striatum in the monkeys using a standard point resolved spectroscopy (PRESS) sequence (TR/TE = 2000/272 ms and 2000/136 ms, 2-kHz sweep width) with presaturation of the water using three chemical shift selective suppression (CHESS) pulses. The voxels were prescribed from a coronal plane and were optimized to cover both caudate and putamen. The voxel sizes ranged from a minimum of $8 \times 8 \times 9$ mm^3 (0.6 cm^3) to a maximum of $1 \times 1 \times 1$ cm^3. Data were analyzed using the NMR1 (New Methods Research, Syracuse New York) software package. After apodization with an exponential multiplication corresponding to a 1–2-Hz line-broadening and Fourier transformation, the major metabolites[30] were integrated in the frequency domain using curve fitting and assuming mixed Lorenzian-Gaussian lineshapes. Metabolite intensities were normalized relative to the phosphocreatine/creatine peak at 3.03 ppm as the denominator.

Acknowledgements

We thank M. Crowley and W. Bucelewicz for technical assistance; grant and facility support were provided by McLean Hospital (USAMRAA DAMD17-98-1-8618) and the New England Regional Primate Research Center (PHS P51RR00168-36).

RECEIVED 5 JUNE; ACCEPTED 11 SEPTEMBER 1998

1. Gjaedde, A. & Wong, D.F. Modeling neuroreceptor binding of radioligands *in vivo*. *Quant. Imaging* 51–79 (1990).
2. Delforge, J. *et al.* Kinetic analysis of central (76)bromolisuride binding to dopamine D2-receptors studied by PET. *J. Cereb. Blood Flow Metab.* **11**, 914–925 (1991).
3. Leenders, K.L. Pathophysiology of movement disorders studied using PET. *J. Neural Transm. Suppl.* **50**, 39–46 (1997).
4. Cruz, C.J., Aminoff, M.J., Meyerhoff, D.J., Graham, S.H. & Weiner, M.W. Proton MR spectroscopic imaging of the striatum in Parkinson's disease. *Magn. Reson. Imaging* **15**, 619–624 (1997).
5. Holshouser, B.A. *et al.* Localized proton NMR spectroscopy in the striatum of patients with idiopathic Parkinson's disease: a multicenter pilot study. *Magn. Reson. Imaging* **33**, 589–594 (1995).
6. Brooks, D.J. PET studies on the early and differential diagnosis of Parkinson's disease. *Neurology* **43**, S6–S16 (1993).
7. Herholz, K. *et al. In vivo* imaging of glucose consumption and lactate concentration in human gliomas. *Ann. Neurol.* **31**, 319–327 (1992).
8. Alger, J.R., Frank, J.L., van Zijl, P.C., Moonen, C.T. & DiChiro, G. Metabolism of human gliomas: assessment with H-1 MR spectroscopy and F-18 fluorodeoxyglucose PET. *Radiology* **177**, 633–641 (1990).
9. Hugg, J.W. *et al.* Elevated lactate and alkalosis in chronic human brain infarction observed by 1H and 31P MR spectroscopic imaging. *J. Cereb. Blood Flow Metab.* **12**, 734–744 (1992).
10. Petroff, O.A. *et al.* Spectroscopic imaging of stroke in humans: histopathology correlates of spectral changes. *Neurology* **42**, 1349–1354 (1992).
11. Prichard, J. *et al.* Lactate rise detected by 1H NMR in human visual cortex during physiologic stimulation. *Proc. Natl. Acad. Sci. USA* **88**, 5829–5831 (1991).
12. Schapira, A.H. Pathogenesis of Parkinson's disease. *Baillieres Clin. Neurol.* **6**, 15–36 (1997).
13. Frost, J.J. *et al.* Positron emission tomographic imaging of the dopamine transporter with 11C-WIN 35,428 reveals marked declines in mild Parkinson's disease. *Ann. Neurol.* **34**, 423–431 (1993).
14. Ehringer, H. & Hornykiewicz, O. Distribution of noradrenaline and dopamine (3-hydroxytyramine) in the human brain and their behavior in diseases of the extrapyramidal system. *Klin. Wochenschr.* **38**, 1236–1239 (1960).
15. Dunnett, S.B., Whishaw, I.Q., Jones, G.H. & Isacson, O. Effects of dopamine-rich grafts on conditioned rotation in rats with unilateral 6-hydroxydopamine lesions. *Neurosci. Lett.* **68**, 127–135 (1986).
16. Ungerstedt, U. 6-Hydroxy-dopamine induced degeneration of central monoamine neurons. *Eur. J. Pharmacol.* **5**, 107–110 (1968).
17. Langston, J.W., Langston, E.B. & Irwin, I. MPTP-induced parkinsonism in human and non-human primates—clinical and experimental aspects. *Acta Neurol. Scand. Suppl.* **100**, 49–54 (1984).
18. Calne, D.D. *et al.* Positron emission tomography after MPTP. *Nature* **317**, 244–248 (1985).
19. Burns, R.S. *et al.* A primate model of parkinsonism: selective destruction of dopaminergic neurons in the pars compacta of the substantia nigra by n-methyl-4-phenyl-1,2,3,6-tetrahydropyridine. *Proc. Natl. Acad. Sci. USA* **80**, 4546–4550 (1983).
20. Hantraye, P. *et al.* In vivo visualization by positron emission tomography of the progressive striatal dopamine receptor damage occuring in MPTP-intoxicated non-human primates. *Life Sci.* **39**, 1375–1382 (1986).
21. Imai, H., Nakamura, T., Endo, K. & Narabayashi, H. Hemiparkinsonism in monkeys after unilateral caudate nucleus infusion of 1-methyl-4-phenyl-1,2,3,6-tetrapyridine (MPTP): behavior and histology. *Brain Res.* **474**, 327–338 (1988).
22. Hantraye, P. *et al.* Dopamine fiber detection by [11 C]-CFT and PET in a primate model of parkinsonism. *Neuroreport* **3**, 265–268 (1992).
23. Wullner, U. *et al.* Dopamine terminal loss and onset of motor symptoms in MPTP-treated monkeys: a positron emission tomography study with 11C-CFT. *Exp. Neurol.* **126**, 305–309 (1994).
24. Temlett, J.A. Parkinson's disease: biology and aetiology. *Curr. Opin. Neurol.* **9**, 303–307 (1996).
25. Frohna, P.A., Rothblat, D.S., Joyce, J.N. & Schneider, J.S. Alterations in dopamine uptake sites and D1 and D2 receptors in cats symptomatic for and recovered from experimental parkinsonism. *Synapse* **19**, 46–55 (1995).
26. Strauss, I., Williamson, J.M., Bertram, E.H., Lothman, E.W. & Fernandez, E.J. Histological and 1H magnetic resonance spectroscopic imaging analysis of quinolinic acid-induced damage to the rat striatum. *Magn. Reson. Med.* **37**, 24–33 (1997).
27. Higuchi, T. *et al.* Effects of severe global ischemia on N-acetylaspartate and other metabolites in the rat brain. *Magn. Reson. Med.* **37**, 851–857 (1997).
28. Jenkins, B., G. *et al.* Non-invasive neurochemical analysis of focal excitotoxic lesions in models of neurodegenerative illness using spectroscopic imaging. *J. Cereb. Blood Flow Metab.* **16**, 450–461 (1996).
29. Guimareaeas, A.R. *et al.* Quantitative nuclear magnetic resonance spectroscopic imaging of neuronal loss in excitotoxic rat brain model. *Neuroscience* **69**, 1093–1101 (1995).
30. Arnold, D.L. *et al.* Use of proton magnetic resonance spectroscopy for monitoring disease progression in multiple sclerosis. *Ann. Neurol.* **36**, 76–82 (1994).
31. Davies, C.A. *et al.* Serial proton magnetic resonance spectroscopy in acute multiple sclerosis lesions. *Brain* **11**, 49–58 (1994).
32. Birken, D.L. & Olendorf, W.H. N-acetyl-L-aspartic acid: a literature review of a compound prominent in 1H-NMR spectroscopic studies of the brain. *Neurosci. Biobehav.* **1**, 23–31 (1989).
33. Urenjak, J., Williams, S.R., Gadian, D.G. & Noble, M. Proton nuclear magnetic resonance spectroscopy unambiguously identifies different neural cell types. *J. Neurosci.* **13**, 981–989 (1993).
34. Brownell, G.L. *et al.* Development in high-resolution positron emission tomography at MGH. *Int. J. Imag. Sys. Technol.* **1**, 207–17 (1989).
35. Derenzo, S.E., Huesman, R.H. & Cahoon, J.L. A positron tomograph with 600 BGO crystals and 2.6 mm resolution. *IEEE Trans. Nucl. Sci.* **NS-35**, 659–664 (1988).
36. Brownell, G.L., Burnham, C.A. & Chesler, D.A. in *The Metabolism of the Human Brain Studied With Positron Emission Tomography,* Ed. (eds. Greitz, T., Ingvar, D.H. & Widen, L.) 13–19 (Raven, New York, 1985).
37. Bugiani, O., Perdelli, F., Salvarani, S., Leonardi, A. & Mancardi, G.L. Loss of striatal neurons in Parkinson's disease: a cytometric study. *Eur. Neurol.* **19**, 339–344 (1980).
38. Hwang, J.H. *et al.* Short echo time proton magnetic resonance spectroscopic imaging of macromolecule and metabolite signal intensities in human brain. *Magn. Reson. Med.* **35**, 633–639 (1996).
39. Frost, J.J. *et al.* Multicompartmental analysis of [11C]-carfentanil binding to opiate receptors in humans measured by positron emission tomography. *J. Cereb. Blood Flow Metab.* **9**, 398–409 (1989).
40. Kaufman, M.J. & Madras, B.K. Severe depletion of cocaine recognition sites associated with the dopamine transporter in parkinson's diseased striatum. *Synapse* **9** (1991).
41. McNeil, T.H., Brown, S.A., Rafols, J.A. & Shoulson, I. Atrophy of medium spiny I striatal dendrites in advanced Parkinson's disease. *Brain Res.* **455**, 148–152 (1988).
42. Federico, F. *et al.* Proton magnetic resonance spectroscopy in parkinson's disease and atypical parkinsonian disorders. *Mov. Disord.* **12**, 903–909 (1997).
43. Clarke, C.E., Lowry, M. & Horsman, A. Unchanged basal ganglia N-acetylaspartate and glutamate in idiopathic parkinson's disease measured by protonmagnetic resonance spectroscopy. *Mov. Disord.* **12**, 297–301 (1997).
44. Carvey, P. *et al.* Alterations in striatal neurotrophic activity induced by dopaminergic drugs. *Pharmacol. Biochem. Behav.* **46**, 195–204 (1993).
45. Brownell, A.-L. *et al.* Cocaine congeners as PET imaging probes for dopamine terminals. *J. Nucl. Med.* **37**, 1186–1192 (1996).
46. Chesler, D.A. Positron emission tomography and three-dimensional reconstruction technique. *Tomograph. Imag. Nuc. Med.* 176–183 (1973).
47. Foster, D.M. *et al.* SAAM II: simulation, analysis and modeling software. *BMES Bull* **18**, 19–21 (1994).